T. RINDFLEISCH*
Jet Propulsion Laboratory
Pasadena, Calif. 91103

Photometric Method for Lunar Topography

Topographic relief can be determined from a single photograph based on knowledge of the surface photometry.

ABSTRACT: *A general and rigorous treatment is given of the photometric method for deriving surface elevation information from a single picture of the surface. In the course of the derivation a brief indication is given of possible photometric function symmetries yielding exact solutions to the problem. It is shown that the photometric properties of the lunar maria are sufficient to produce an exact solution but with an inherent practical difficulty. The resulting equations are then specialized to the case of lunar photography and applied to the Ranger pictures as part of a digital processing procedure. Examples of the resulting elevation maps are given.*

INTRODUCTION

QUANTITATIVE ELEVATION INFORMATION about a surface can be derived from pictures both by stereoscopic and by photometric methods. The second method, which is of interest here, was first suggested by van Diggelen (Ref. 1) in 1951. Extending his original formulation of the problem, it is desired to reconstruct quantitatively the shape of a surface being photographed using the imaging geometry, the facsimile system transfer characteristics, and the surface photometric properties. A rigorous solution to this problem is presented and the results are applied to the lunar pictures taken by the three Ranger impacting spacecraft.

CALCULATION OF ELEVATIONS IN TERMS OF A LENS-CENTERED COORDINATE SYSTEM

The pertinent photometry of extended surfaces can be summarized as follows. For simplicity, it will be assumed that the surface possesses homogenous photometric properties at least over the local area under consideration. The photometric geometry can be completely defined in terms of three angles; the incidence angle i (angle between the direction of incident light and the surface normal), the emission angle e (angle between the direction of emitted light and the surface normal), and the phase angle g (angle between the directions of incident and emitted light). This geometry is shown in Figure 1. For uniform collimated illumination of the surface, such as with sunlight, the luminence b can be written

$$b(i, e, g) = \rho_0 E_0 \phi(i, e, g) \tag{1}$$

where ρ_0 is the normal albedo of the surface, E_0 is the uniform illumination intensity, and ϕ (i, e, g) is the surface photometric function. The normalization of ϕ is such that

$$\phi(0, 0, 0) = 1.$$

* This paper presents the results of one phase of research conducted at J.P.L., California Institute of Technology, under Contract No. NAS 7-100, sponsored by NASA. The paper has been cleared for United States publication by the Technical Information Section, J.P.L. A form of the paper has appeared as a copyrighted J.P.L. Laboratory Technical Report No. 32-786, September 15, 1965.

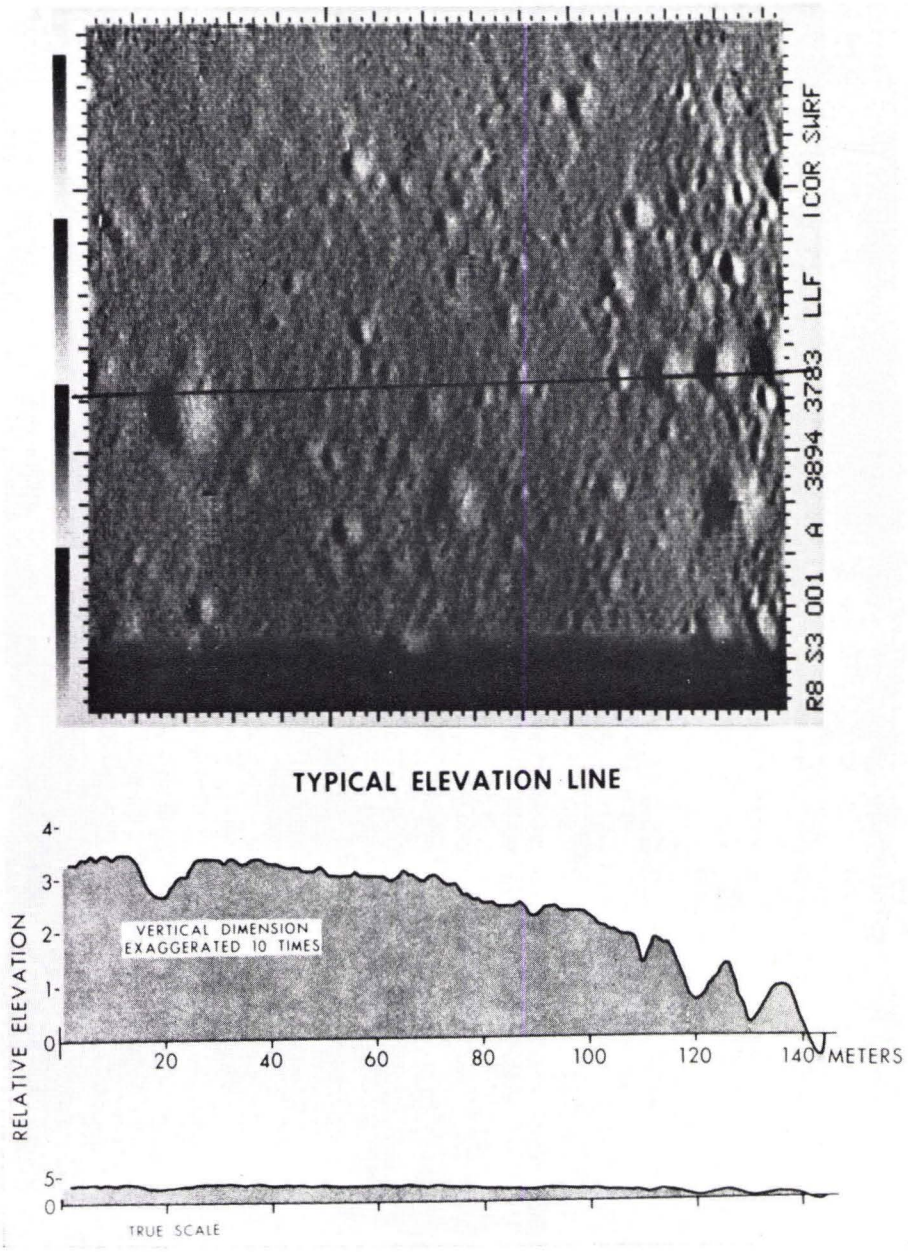

FRONTISPIECE. Elevation profile through the last P-3 picture from Ranger VIII.

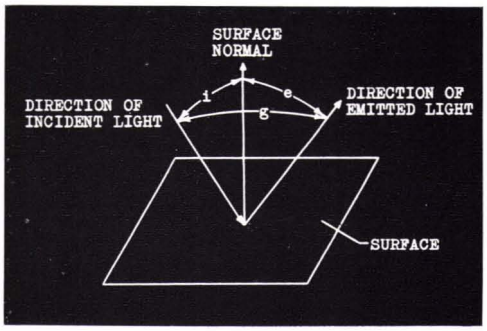

FIG. 1. Surface Photometric Geometry

NOMENCLATURE

- b Surface luminance.
- e Emission angle for surface photometric geometry.
- E_0 Solar constant.
- F Focal length of lens.
- g Phase angle for surface photometric geometry.
- h Height of point in object space above spherical datum which is assumed to locally approximate a plane.
- i Incidence angle for surface photometric geometry.
- J Jacobian of imaging transformation.
- $\hat{N}$ Unit vector normal to object surface.
- $\hat{N}_0$ Unit vector normal to plane containing zero phase point and center of lens.
- P,P_0 Points on path S' in image plane.
- r Length of position vector $\boldsymbol{r}$.
- r' Length of position vector $\boldsymbol{r}'$.
- r_c Length of $\boldsymbol{r}_c$.
- $\boldsymbol{r}$ Position vector from center of lens to point in object space.
- $\hat{r}$ Unit vector from center of lens toward point in object space.
- $\boldsymbol{r}'$ Position vector from center of lens to point in image space.
- $\hat{r}'$ Unit vector from center of lens toward point in image space.
- $\boldsymbol{r}_c$ Position vector from center of lens to object point on spherical datum which is imaged at center of output format.
- $\hat{r}_c$ Unit vector along $\boldsymbol{r}_c$.
- $\boldsymbol{r}_M$ Position vector from center of lens to center of spherical body.
- R Length of $\boldsymbol{R}$.
- R_0 Radius of spherical datum.
- $\boldsymbol{R}$ Position vector from center of body to point in object space.
- $\hat{R}_c$ Unit vector normal to spherical datum at object point which is imaged at center of output format.
- $\hat{R}_i$ Unit vector from surface toward light source.
- s' Path length variable along path S'.
- S' Path in image plane.
- $\hat{S}_T'$ Unit vector tangent to path S'.
- x,y,z Coordinates of point in object space with respect to lens-centered coordinate system.
- x',y',z' Coordinates of point in image space with respect to lens-centered coordinate system.
- $\hat{x},\hat{y},\hat{z}$ Unit vectors along principal axes of right-handed Cartesian lens-centered coordinate system; $\hat{z}$ is along optical axis.
- α Projection of emission angle e in plane containing g for surface photometric geometry.
- ρ_0 Surface normal albedo.
- $\phi(i,e,g)$ Surface photometric function.
- ∇ Nabla or gradient operator with respect to unprimed coordinates.
- ∇' Nabla or gradient operator with respect to primed coordinates.

Consider now an enumeration of the information known about the output scene reproduction and the geometry of its formation. The output reproduction may be a photographic print or transparency, or simply a magnetic tape recording of the video information from which, of course, it is assumed that the proper two-dimensional geometric relationship of the signals can be derived. It is assumed that the static or uniform field transfer function of the facsimile system is known, so that an output signal, be it the print reflectance, the transparency transmittance, or the tape voltage output, is directly relatable to the object scene luminance. This relationship is not quite so simple since the reproduction process is not perfect, i.e., the input scene image is degraded by the facsimile system, so that an output signal is not truly related to the input luminance through the uniform field transfer function. This is particularly true for steep luminance gradients, e.g., in small surface features. For the present, however, it is assumed that these degradations have been corrected by digital

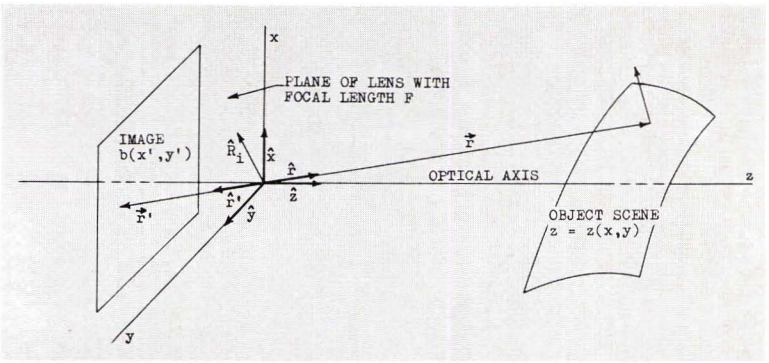

FIG. 2. Viewing geometry in a lens-centered coordinate system.

processing methods or by spatial filtering, so that the reproduction system may be considered perfect and the uniform field transfer function indeed applies. In this case, the output reproduction can just as well be considered as a two-dimensional array of luminances corresponding to the input scene.

To be more specific, let a right-handed Cartesian coordinate system be located with its origin at the center of the image-forming lens and with the lens in the xy-plane (see Figure 2). With the convention that primed coordinates refer to points in image space and unprimed coordinates refer to points in object space, the output facsimile can be considered as an array of luminances $b(x', y')$. From the image-forming process and the known coordinates of points in the image plane, one knows the direction $\hat{r}'$ from every object scene point to its image.[1] This follows since for a simple lens, the position vector $\boldsymbol{r}'$ of the image of an object point with position vector $\boldsymbol{r}$ is given by (assuming distant objects)

$$\boldsymbol{r}' = -\frac{F}{\boldsymbol{r}\cdot\hat{z}}\boldsymbol{r} \tag{2}$$

Here F is the focal length of the lens and $\hat{z}$ is a unit vector along the optical axis normal to the image plane. The distant object assumption is formally written

$$\boldsymbol{r}\cdot\hat{z} \gg F$$

Moreover, one knows the direction of incident illumination on the scene. This direction is denoted by a unit vector $\hat{R}_i$ directed toward the light source. Thus, the phase angle g is known for every point in the image since

$$g = \cos^{-1}(\hat{r}'\cdot\hat{R}_i), \qquad 0 \leq g \leq \pi \tag{3}$$

and so with every $b(x', y')$ in the output array is associated a $g(x', y')$. Furthermore at every point (x', y') in the image plane one obtains a relationship between the incidence angle i and the emission angle e through Equation 1 where the relationship is

$$b(x', y') = \rho_0 E_0 \phi[i, e, g(x', y')]. \tag{4}$$

This relationship between i and e defines the equations of contours on the photometric function surface for given g such that $\phi = b(x', y')/\rho_0 E_0$. Hence there are many possible surface normal orientations all giving the same observed luminance. It will be shown later that the solution to the present problem is intimately related to the nature of these contours.

[1] A letter in boldface indicates a vector of, in general, non-unit length. A caret over a letter indicates a unit vector.

Therefore, the totality of information available in the image may be summarized as follows:

F	The focal length of the lens.
$\hat{z}$	The direction of the optical axis.
$\hat{R}_i$	The direction of incident illumination.
$\hat{r}'$	The direction from an object point to its image.
$b(x', y')$	The object scene luminance corresponding to each image point
$g(x', y')$	The phase angle for every point in the image plane.
$\{i(x', y'), e(x', y')\}$	The locus of allowed incidence and emission angles producing the same $b(x', y')$ for the known $g(x', y')$.

Consider now a representation of the object scene from which one can write down the necessary analysis. Since the lens-centered coordinate system is already available and is of particular pertinence to this part of the problem, a representation in terms of it will be used. A coordinate system convenient to the surface being photographed is of perhaps more interest for surface interpretation and will be introduced later. In the lens-centered coordinate system, an equation for the object scene can be written (see Figure 2)

$$z = z(x, y) \tag{5}$$

where, of course, the functional form of the expression is to be determined. From the picture, lateral (x, y) geometric information can be derived about the scene. It remains to determine the distance z and ultimately the length r of the position vector to points on the object surface. This problem can be usefully stated as trying to find some path S' with a path length variable s' along it in the output picture such that the derivative dz/ds' can be written as a function of the known picture information. Then since the position vector $\boldsymbol{r}$ to an object point can be written in terms of $z(x, y)$ and $\hat{r}'$, an expression for dr/ds' can be determined similarly as a function f of the known picture data:

$$\frac{d\boldsymbol{r}}{ds'} = f(F, \hat{z}, \hat{R}_i, \hat{r}', g, \{i, e\}). \tag{6}$$

So if one knows the length r_0 of an object position vector for some point on the path, this differential equation can be integrated to find r and finally $\boldsymbol{r}$ everywhere along the path, thereby reconstructing a portion of the object surface. What follows is aimed at this goal.

Let the path S' in the image have a parametric representation

$$\begin{aligned} x' &= x'(s') \\ y' &= y'(s'). \end{aligned} \tag{7}$$

Then considering z to be a function of x' and y', one can write

$$\frac{dz}{ds'} = \nabla' z \cdot \hat{S}_T' \tag{8}$$

where ∇' is the nabla or gradient operator with respect to the primed coordinates,

$$\nabla' = \left(\frac{\partial}{\partial x'}\right)_{y'z'} \hat{x} + \left(\frac{\partial}{\partial y'}\right)_{x'z'} \hat{y} + \left(\frac{\partial}{\partial z'}\right)_{x'y'} \hat{z}; \tag{9}$$

$\hat{x}$, $\hat{y}$, and $\hat{z}$ are unit vectors along the principal Cartesian axes; and $\hat{S}_T'$ is a unit vector

tangent to the path S',

$$\hat{S}_{T'} = \frac{dx'}{ds'}\,\hat{x} + \frac{dy'}{ds'}\,\hat{y}. \tag{10}$$

Changing to the object space variables x and y, the derivatives $(\partial z/\partial x')_{y'}$ and $(\partial z/\partial y')_{x'}$ must be calculated. Using the chain rule one has

$$\left(\frac{\partial z}{\partial x'}\right)_{y'} = \left(\frac{\partial z}{\partial x}\right)_{y}\left(\frac{\partial x}{\partial x'}\right)_{y'} + \left(\frac{\partial z}{\partial y}\right)_{x}\left(\frac{\partial y}{\partial x'}\right)_{y'}$$

$$\left(\frac{\partial z}{\partial y'}\right)_{x'} = \left(\frac{\partial z}{\partial x}\right)_{y}\left(\frac{\partial x}{\partial y'}\right)_{x'} + \left(\frac{\partial z}{\partial y}\right)_{x}\left(\frac{\partial y}{\partial y'}\right)_{x'}. \tag{11}$$

The derivatives $(\partial x/\partial x')_{y'}$, $(\partial y/\partial x')_{y'}$, $(\partial x/\partial y')_{x'}$, and $(\partial y/\partial y')_{x'}$ are calculated using the imaging formula in Equation 2. Specifically let

$$x' = \xi(x, y) = -\frac{Fx}{z(x, y)}$$

$$y' = \eta(x, y) = -\frac{Fy}{z(x, y)}. \tag{12}$$

Using some more or less advanced calculus, one can show that

$$\left(\frac{\partial x}{\partial x'}\right)_{y'} = \frac{(\partial\eta/\partial y)_x}{J}; \qquad \left(\frac{\partial y}{\partial x'}\right)_{y'} = -\frac{(\partial\eta/\partial x)_y}{J}$$

$$\left(\frac{\partial x}{\partial y'}\right)_{x'} = -\frac{(\partial\xi/\partial y)_x}{J}; \qquad \left(\frac{\partial y}{\partial y'}\right)_{x'} = \frac{(\partial\xi/\partial x)_y}{J} \tag{13}$$

where J is the Jacobian

$$J = \begin{vmatrix} (\partial\xi/\partial x)_y & (\partial\xi/\partial y)_x \\ (\partial\eta/\partial x)_y & (\partial\eta/\partial y)_x \end{vmatrix} \neq 0$$

From the definitions of $\xi(x, y)$ and $\eta(x, y)$ in Equation 12 one can show that the Jacobian is given by

$$J = \frac{F^2}{z^3}\left[z - x\left(\frac{\partial z}{\partial x}\right)_y - y\left(\frac{\partial z}{\partial y}\right)_x\right]. \tag{14}$$

Now if a three dimensional surface has a representation

$$G(x, y, z) = 0,$$

a unit normal $\hat{N}$ to the surface at the point (x, y, z) is given by

$$\hat{N} = \frac{\nabla G(x, y, z)}{|\nabla G(x, y, z)|}$$

where ∇ is the nabla or gradient operator with respect to the unprimed coordinates. In the present case with the surface represented by (see Equation 5)

$$z - z(x, y) = 0,$$

one can show that

$$\hat{N} = (\hat{N}\cdot\hat{z})[\hat{z} - \nabla z(x, y)]. \tag{15}$$

Noting that, by definition,

$$\boldsymbol{r} = x\hat{x} + y\hat{y} + z(x, y)\hat{z}$$

one has using Equation 15 and Equation 14 for the Jacobian

$$J = \frac{F^2}{z^3}\frac{\hat{N}\cdot\boldsymbol{r}}{\hat{N}\cdot\hat{z}} \tag{16}$$

where $J \neq 0$ implies that $\hat{N}\cdot\boldsymbol{r} \neq 0$. Then using Equations 16, 13, 12, and 11, one can easily show that

$$\nabla' z(x, y) = -\frac{z(x, y)}{F}\frac{(\hat{N}\cdot\hat{z})(\hat{r}\cdot\hat{z})}{(\hat{N}\cdot\hat{r})}\nabla z(x, y). \tag{17}$$

Finally from Equation 15

$$\nabla z(x, y) = \hat{z} - \frac{\hat{N}}{\hat{N}\cdot\hat{z}}$$

so that from Equation 17

$$\nabla' z(x, y) = -\frac{z(x, y)}{F}\frac{(\hat{N}\cdot\hat{z})(\hat{r}\cdot\hat{z})}{(\hat{N}\cdot\hat{r})}\left[\hat{z} - \frac{\hat{N}}{\hat{N}\cdot\hat{z}}\right]. \tag{18}$$

Then the desired expression for dz/ds' in terms of the surface normal is, using Equations 8 and 18,

$$\frac{dz}{ds'} = \frac{z(x, y)}{F}\frac{(\hat{N}\cdot\hat{S}_T')(\hat{r}'\cdot\hat{z})}{(\hat{N}\cdot\hat{r}')} \tag{19}$$

where the substitution $\hat{r} = -\hat{r}'$ has been made.

To reconstruct the object scene one needs to know the position vector $\boldsymbol{r}$ to each of its points. From the imaging geometry (Equation 2), the direction of $\boldsymbol{r}$ is given by $-\hat{r}'$ so that only the length r must be determined. Assuming $z(x, y)$ to be known, $\boldsymbol{r}$ can be written

$$\boldsymbol{r} = \frac{z(x, y)}{\hat{r}'\cdot\hat{z}}\hat{r}'$$

and its length is

$$r = -\frac{z(x, y)}{\hat{r}'\cdot\hat{z}}. \tag{20}$$

Thus a differential equation for r can be written as,

$$\frac{dr}{ds'} = -\frac{1}{\hat{r}'\cdot\hat{z}}\frac{dz}{ds'} + \frac{z(x, y)}{(\hat{r}'\cdot\hat{z})^2}\frac{d(\hat{r}'\cdot\hat{z})}{ds'}$$

and it is easy to show that

$$\frac{dr}{ds'} = -\frac{1}{\hat{r}'\cdot\hat{z}}\left[\frac{dz}{ds'} - \frac{z(x, y)}{F}(\hat{r}'\cdot\hat{z})(\hat{r}'\cdot\hat{S}_T')\right]. \tag{21}$$

Substituting Equation 19 in Equation 21 it follows that

$$\frac{dr}{ds'} = \frac{r}{F}\frac{(\hat{r}'\cdot\hat{z})}{(\hat{N}\cdot\hat{r}')}[\hat{r}'\times(\hat{N}\times\hat{r}')]\cdot\hat{S}_T'. \tag{22}$$

It remains to calculate the surface normal $\hat{N}$ in terms of the photometric geometry and thence to write Equation 22 in terms of known quantities as in Equation 6. For this purpose consider a partially orthogonal coordinate system with axes along the unit vectors $\hat{r}'$, $\hat{R}_i$ and $\hat{R}_i\times\hat{r}'/\sin g$ where it is assumed that $g\neq 0$ (see Figure 3). It is straightforward to show that in this coordinate system $\hat{N}$ can be written

$$\hat{N} = \frac{1}{\sin^2 g}[(\cos e - \cos i\cos g)\hat{r}' + (\cos i - \cos e\cos g)\hat{R}_i \pm \sqrt{\sin^2 g - \cos^2 i - \cos^2 e + 2\cos i\cos e\cos g}\,(\hat{R}_i\times\hat{r}')] \tag{23}$$

where the plus or minus sign in the last term represents the inherent ambiguity in the orientation of $\hat{N}$. Substituting Equation 23 in Equation 22 it follows that

$$\frac{dr}{ds'} = \frac{r}{F}\frac{(\hat{r}'\cdot\hat{z})}{\sin^2 g}\left[\left(\frac{\cos i}{\cos e} - \cos g\right)[\hat{r}'\times(\hat{R}_i\times\hat{r}')] \pm \sqrt{\frac{\sin^2 g}{\cos^2 e} - 1 - \frac{\cos^2 i}{\cos^2 e} + 2\frac{\cos i}{\cos e}\cos g}\,(\hat{R}_i\times\hat{r}')\right]\cdot\hat{S}_T' \tag{24}$$

which is an equation essentially in the form of Equation 6.

Unfortunately as discussed earlier, knowing the luminance b and phase angle g over the picture only establishes a relationship between i and e at each point of the picture through Equation 4. Clearly a detailed knowledge of both i and e at each picture point is needed in Equation 24 as it stands. However, it will be noted that the path S' and hence the vector $\hat{S}_T'$ are still arbitrary. The path can be chosen to form any linear combination of the two terms in Equation 24 through the direction of $\hat{S}_T'$ depending on the particular photometric function symmetries under consideration. A case of particular interest for lunar photography results from eliminating the second term. This path definition can be formally written

$$(\hat{R}_i\times\hat{r}')\cdot\hat{S}_T' = 0 \tag{25}$$

and in this case Equation 24 becomes

$$\frac{dr}{ds'} = \frac{r}{F}\frac{(\hat{r}'\cdot\hat{z})}{\sin^2 g}\left(\frac{\cos i}{\cos e} - \cos g\right)[\hat{r}'\times(\hat{R}_i\times\hat{r}')]\cdot\hat{S}_T'. \tag{26}$$

Clearly the choice of the path in Equation 25 has yielded an exact solution to the present problem only for photometric functions which for a given phase angle g yield constant luminances for constant $\cos i/\cos e$. One must be able to write

$$b(i, e, g) = \rho_0 E_0 \phi(g, \cos i/\cos e). \tag{27}$$

It is straightforward to show that the loci of constant $\cos i/\cos e$ are meridians in a spherical coordinate system whose equator contains the vectors $\hat{R}_i$ and $\hat{r}'$. Thus for this symmetry property a more convenient choice of photometric angles is as shown in Figure 4. The photometric geometry is completely defined by the phase angle g and a new angle α taken to be the angle between the component of $\hat{N}$ in the plane containing g and the direction $\hat{r}'$. The angle α ranges from $-\pi/2$ to $\pi/2$ and is considered positive if it does not overlap the angle g and negative if it does, as in Figure 4.

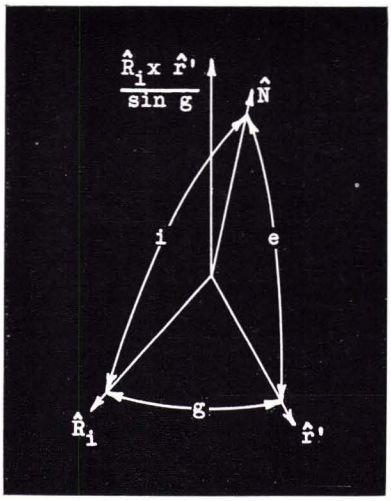

FIG. 3. Decomposition of Surface Normal in Terms of Photometric Angles

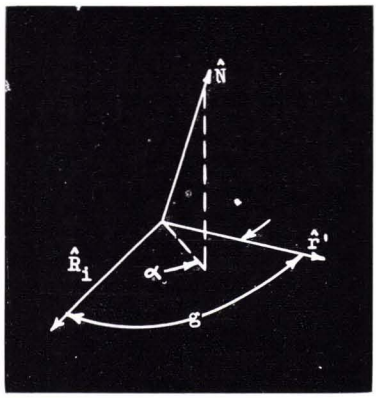

FIG. 4. Photometric Angle Definitions for cos i/cos e Symmetry

Then Equation 27 becomes

$$b(g, \alpha) = \rho_0 E_0 \phi(g, \alpha). \tag{28}$$

Physically Equation 28 places fairly severe restrictions on the properties of the surface being viewed. For zero phase angle, the incidence and emission angles are identical irrespective of the orientation of the surface normal. Thus at zero phase a body of any shape would appear uniformly bright implying that the surface is highly backscattering. It is not clear how widespread such a photometric property might be for celestial and terrestrial surfaces but measurements show that it applies to the maria on the moon (Reference 2). This fortunate circumstance offers a promising way to deduce elevation maps of the lunar surface from spacecraft photography containing little stereoscopic data. This will be discussed in more detail later.

Using the g and α notation for the photometric geometry (under the above symmetry requirements) it can be shown that Equation 26 reduces to

$$\frac{dr}{ds'} = -\frac{r}{F}\frac{(\hat{r}' \cdot \hat{z})}{\sin g} \tan \alpha [\hat{r}' \times (\hat{R}_i \times \hat{r}')] \cdot \hat{S}_T' \tag{29}$$

where the path condition in Equation 25 still applies. Furthermore one can show that Equation 25 defines a family of straight-line paths in the image plane all of which pass through the image point for which $\hat{r}' = \hat{R}_i$ (see Figure 5). This image point corresponds to an object point for which the photometric geometry gives a phase angle of zero and will be called the "zero phase point." A useful way of describing the family of paths defined by Equation 25 is as the family of intersections with the focal plane of the set of planes passing through the zero phase point and the center of the image-forming lens. Clearly any one of these paths can be specified by the normal $\hat{N}_0$ to its generating plane. So for a particular plane with normal $\hat{N}_0$ and corresponding path $S'(\hat{N}_0)$, one can write $\hat{N}_0$ as

$$\hat{N}_0 = \frac{\hat{R}_i \times \hat{r}'}{\sin g} \tag{30}$$

where $\hat{r}'$ corresponds to any image point along $S'(\hat{N}_0)$ except the zero phase point and the sign of $\hat{N}_0$ is arbitrarily defined by Equation 30. Then since $\hat{S}_T'(\hat{N}_0)$ is normal

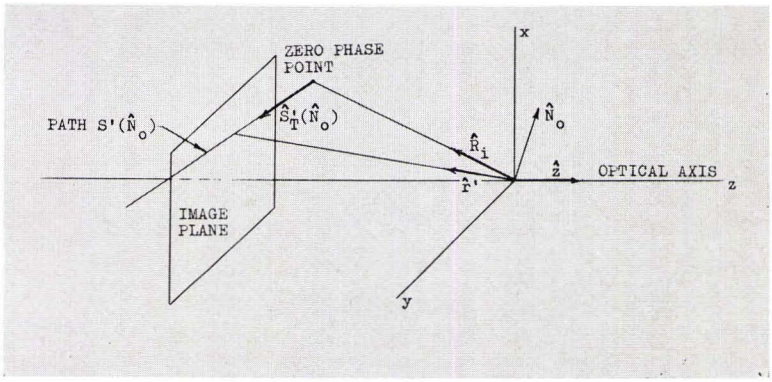

FIG. 5. Integration path vector conventions.

to $\hat{N}_0$ by Equation 25 and since $\hat{S}_T'(\hat{N}_0)$ is also normal to $\hat{z}$ (direction of the optical axis), one can write

$$\hat{S}_T'(\hat{N}_0) = \frac{\hat{z} \times \hat{N}_0}{|\hat{z} \times \hat{N}_0|} \tag{31}$$

where the direction of $\hat{S}_T'(\hat{N}_0)$ is along the path $S'(\hat{N}_0)$ and away from the zero phase point (see Figure 5). Finally substituting Equation 31 in Equation 29 one obtains as the final differential equation for the present special case,

$$\frac{dr}{ds'} = -\frac{r}{F} \frac{(\hat{r}' \cdot \hat{z})^2}{|\hat{z} \times \hat{N}_0|} \tan \alpha \tag{32}$$

This is a particularly simple differential equation. Since F, $\hat{z}$, and $\hat{N}_0$ are constants along the path and $\hat{r}'$ and α are known as functions of s' (α comes from Equation 28 through the known b, g, and the assumed photometric function symmetries), the solution is simply

$$\frac{r(P)}{r(P_0)} = \exp\left[\frac{-1}{F|\hat{z} \times \hat{N}_0|} \int_{P_0}^{P} (\hat{r}' \cdot \hat{z})^2 \tan \alpha \, ds'\right] \tag{33}$$

where s' is measured positive away from the zero phase point, and P and P_0 are points along the path of integration.

It may be useful at this point to list the symbols found in Equation 33 and their definitions. For some integration path, a straight line in the image plane passing through the zero phase point (the image point, for which the photometric geometry gives a phase angle of zero), the symbols mean:

P, P_0	Points along the integration path; P_0 is the reference point for the integral.
$r(P)$, $r(P_0)$	The lengths of the position vectors to the object points corresponding to the image points P and P_0.
F	The focal length of the imaging lens.
$\hat{z}$	A unit vector along the optical axis.
$\hat{N}_0$	A unit normal to the plane generating the integration path.
$\hat{r}'$	A unit vector from the center of the lens to a point on the integration path.
α	The auxiliary photometric angle determined from the object scene luminance and the phase angle g through the photometric function (assumed to possess the cos i/cos e symmetry).

s' A path length variable along the integration path and measured positive away from the zero phase point.

To summarize the results obtained so far, an equation has been derived (Equation 24) which is a differential equation for an object surface in terms of quantities derivable from a single picture. The differential equation is applicable along an arbitrary path through the image plane. Unfortunately the equation in general requires an impossible amount of information from the surface photometric function. The path can be chosen, however, to eliminate terms which cannot be calculated depending on the photometric function symmetry. In particular, the equation was specialized to the case of lunar photography. The resulting equation (Equation 33) relates the lengths of position vectors of points on the object surface to the presumably known length of one of the position vectors along any straight-line path in the image plane passing through the zero phase point. Clearly then, if the zero phase point lies within the picture all of the position vector lengths can be related to the one for that point. Unfortunately, the zero phase point is undesirable to photograph since only details due to nonuniformities in the surface albedo are visible (assumed nonexistent in the present treatment) because of the lunar photometric properties. Thus, in practical applications of this method of extracting surface elevation data, one can relate elevations only along disconnected paths through the image. There are several possible ways of relating the elevations from one path to another. These are respectively: (1) using another picture of the surface such that the integration paths cross those of the first picture; (2) using stereoscopic data which again requires a second picture; and (3) using the requirement that the surface be locally smooth and essentially flat. The third method preserves the requirement of only one picture of the surface but must ignore surface tilts in the direction normal to the integration paths.

Calculation of Elevations in Terms of a Surface-Centered Coordinate System

As mentioned earlier, surface interpretations are far simpler in terms of a coordinate system convenient to the surface. The case which will be discussed here is that of a camera system photographing a spherical body such as the moon. The camera will be assumed distant from the surface compared to the surface fluctuations about a datum but with a field of view small enough that curvature can be neglected. The problem is then to represent the surface in terms of elevations above some reference datum which approximates a plane.

Let $\boldsymbol{r}_M$ be the position vector of the center of the spherical body in the lens-centered coordinate system (see Figure 6). Then if an object point has a position vector $\boldsymbol{r}(P)$ in the lens-centered coordinate system (P is the corresponding point in the image plane), and $\boldsymbol{R}(P)$ in a body-centered coordinate system, one has

$$\boldsymbol{R}(P) = \boldsymbol{r}(P) - \boldsymbol{r}_M. \tag{34}$$

Since over the field of view the spherical datum is assumed to approximate a plane, the position vectors $\boldsymbol{R}$ of the object points relative to the body center have essentially the same direction. This direction is taken to be normal to the spherical datum at the point corresponding to the center of the output picture. Note that the center of the picture need not be where the optical axis intersects the image plane, e.g., in television systems where the raster can be displaced. Let the center of the picture be at a direction $\hat{r}_c'$ from the center of the lens and let r_c be the length of the position vector to the corresponding point on the spherical datum of radius R_0. Then it can be shown that

$$r_c = -(\hat{r}_c' \cdot \boldsymbol{r}_M) - [R_0^2 + (\hat{r}_c' \cdot \boldsymbol{r}_M)^2 - \boldsymbol{r}_M \cdot \boldsymbol{r}_M]^{1/2}$$

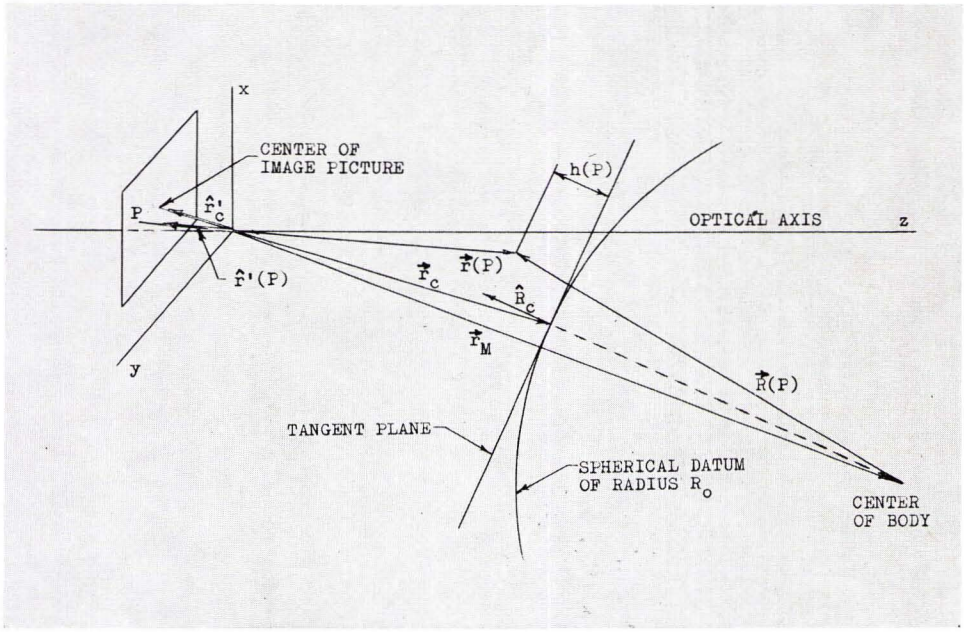

FIG. 6. Geometry of camera relative to spherical body.

and the normal $\hat{R}_c$ to the datum at this point is (see Figure 6)

$$\hat{R}_c = -\frac{1}{R_0}(r_c\hat{r}_c' + \mathbf{r}_M).$$

Then the height $h(P)$ of the object point at $\mathbf{r}(P)$ above the datum is

$$h(P) \approx \mathbf{r}(P)\cdot\hat{R}_c - \mathbf{r}_c\cdot\hat{R}_c$$

where $\mathbf{r}_c = -r_c\hat{r}_c'$.

Now P falls on some integration path S' described earlier, so that only the quantity $r(P)/r(P_0)$ is known from Equation 33 where P_0 is a reference point along the path. The reference position vector length $r(P_0)$ is not accurately known except that it corresponds to an object point assumed close to the reference datum compared to the camera distance. Thus Equation 35 can be written

$$h(P) \approx [\mathbf{r}(P_0)\cdot\hat{R}_c]\frac{r(P)}{r(P_0)}\frac{[\hat{r}'(P)\cdot\hat{R}_c]}{[\hat{r}'(P_0)\cdot\hat{R}_c]} - \mathbf{r}_c\cdot\hat{R}_c$$

and finally to first order in small quantities

$$h(P) \approx -(\mathbf{r}_c\cdot\hat{R}_c)\left\{1 - \frac{r(P)}{r(P_0)}\frac{[\hat{r}'(P)\cdot\hat{R}_c]}{[\hat{r}'(P_0)\cdot\hat{R}_c]}\right\} + \Delta h(P_0). \tag{36}$$

Consistent with the previous results, since $\Delta h(P_0)$ involves the unknown $r(P_0)$ for an integration path, only a relative height given by the first term in Equation 36 can be found. Due to the linearization procedure inherent in the present approximations, the relative elevations about the body datum differ from the actual values by an additive constant $\Delta h(P_0)$, which depends only on the path. This is in contrast to the ratios of values obtained in the analysis resulting in Equation 33.

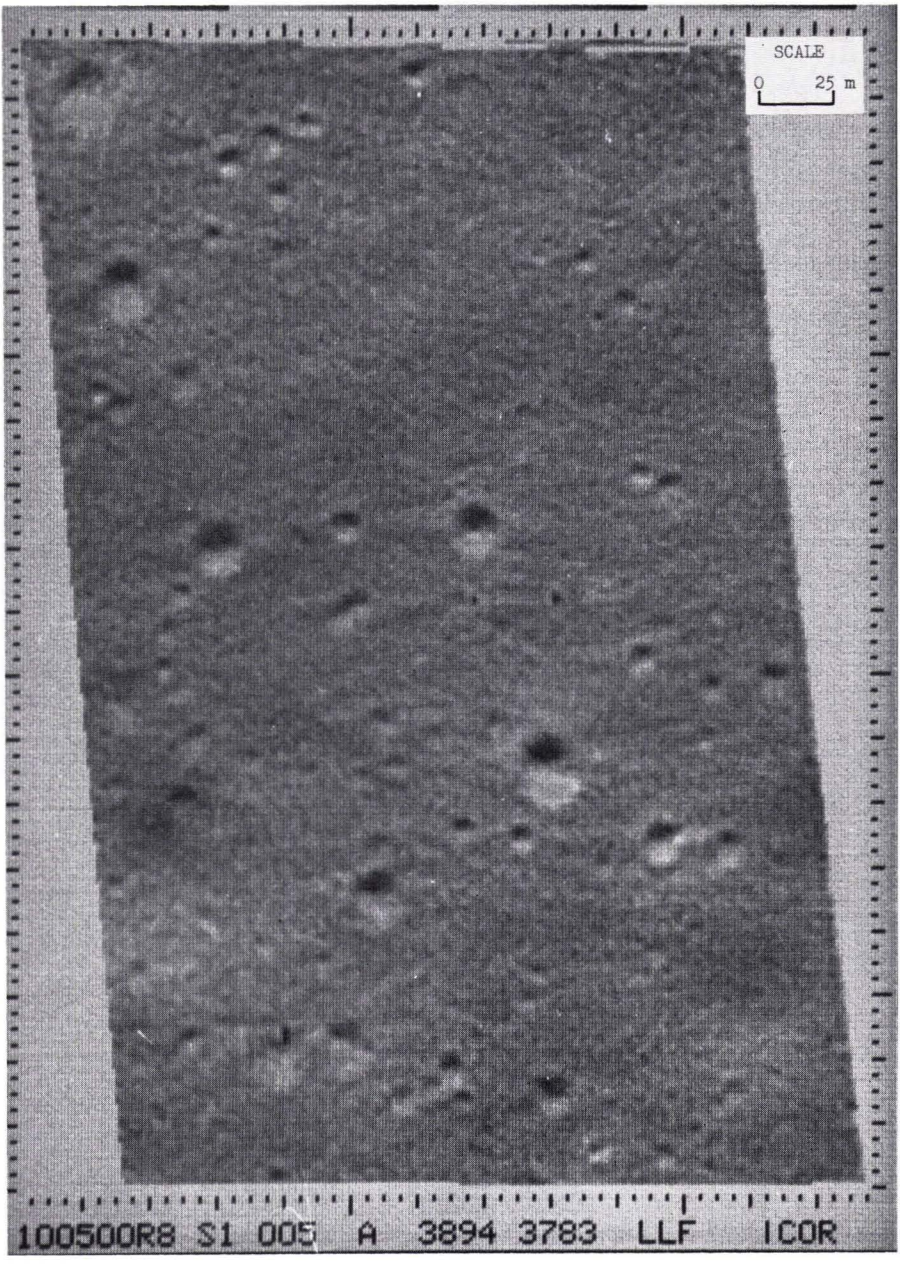

FIG. 7. Corrected and rectified P-1 picture (1005) from Ranger VIII.

APPLICATION TO THE RANGER PICTURES

The above analysis specialized to the lunar photometric properties offers a promising method for deriving lunar topographic information from spacecraft pictures. In particular the Ranger pictures of the moon have little stereoscopic coverage so that the present photometric method is the only way to derive topographic maps.

The necessary calculations lend themselves quite nicely to digital computation and were incorporated in the digital picture processing program currently being

developed at the Jet Propulsion Laboratory. Since the zero phase point never appears in the Ranger pictures for reasons discussed above, and since no stereoscopic data exists in general, an assumption to relate relative elevations across the integration paths is needed. For a complex picture with much detail, short of manipulating the relative elevations by hand, this assumption must be statistical in nature. The simplest assumption and one difficult to improve upon without extreme complication, is that the average elevations along the respective integration paths are all equal. This assumption obviously relies for accuracy on the existence of many random elevation fluctuations along each path and neglects any general slope of the surface in a direction normal to the paths. Such a slope is not detectable from a single picture by these methods due to the lunar photometric properties and must be measured by stereoscopy.

Using this assumption to relate relative elevations across the integration paths, a topographic map of the area covered by a picture can be calculated. Examples of the results of this procedure are shown in the Frontispiece and Figures 7 and 8. The Frontispiece shows the last P-3 frame from Ranger VIII in an unrectified form with certain noises removed and with the sine-wave response fall-off of the camera corrected by digital computer processing. Below the picture is an elevation profile along the line shown in the picture, depicted at 10 times vertical exaggeration and at true scale. It can be seen that the profile follows the picture shadings very well. Analysis of the profile taking into account the lighting direction when the picture was taken, gives good agreement with the shadow areas actually found in the picture. Figure 7 shows a rectified picture of the fifth from the last P-1 frame from Ranger VIII with the same noises removed and with the same sine-wave response correction applied. Figure 8 then shows the same frame as Figure 7 in the form of a complete contoured elevation map. The horizontal scales are as shown in Figures 7 and 8 and the contours are lettered according to the legend shown. It will be noted that the contours are quite consistent with a subjective interpretation of the brightness picture in Figure 7 in terms of elevations. Again the shadow analysis of the contour map gives good agreement with the picture.

Conclusions

A solution has been found to the original problem, namely the derivation of quantitative topographic information about an object scene using a single picture of it and a knowledge of the surface photometry. The specific solution valid for the lunar photometric properties was extracted from a more general equation. Clearly other photometric properties than those of the moon will give exact solutions but this problem requires detailed study. The consideration of the solution for the lunar case was motivated by the original purpose of this work, i.e., to derive lunar topographic data from the Ranger pictures of the moon. Not having stereoscopic coverage for the highest resolution frames, the present photometric method is the only way of accomplishing this goal.

The subject of accuracy is extremely important. Unfortunately, one will not be able to visit the moon to verify the derived Ranger maps for some time. In addition the details of processing a picture from raw data to final contour map are such that it seems unrealistic to try to estimate the errors analytically. One is thus left to indirect estimates or specific attempts to reconstruct a known scene. The latter method has not been attempted yet, but the former method has to some extent. The fact that shadow studies show good agreement with results as discussed with Figure 7, and the fact that contours are internally consistent and are easily interpreted in terms of picture shadings is very promising. Clearly the assumption of uniform albedo is unrealistic for large areas, but is not a necessary assumption to the analysis.

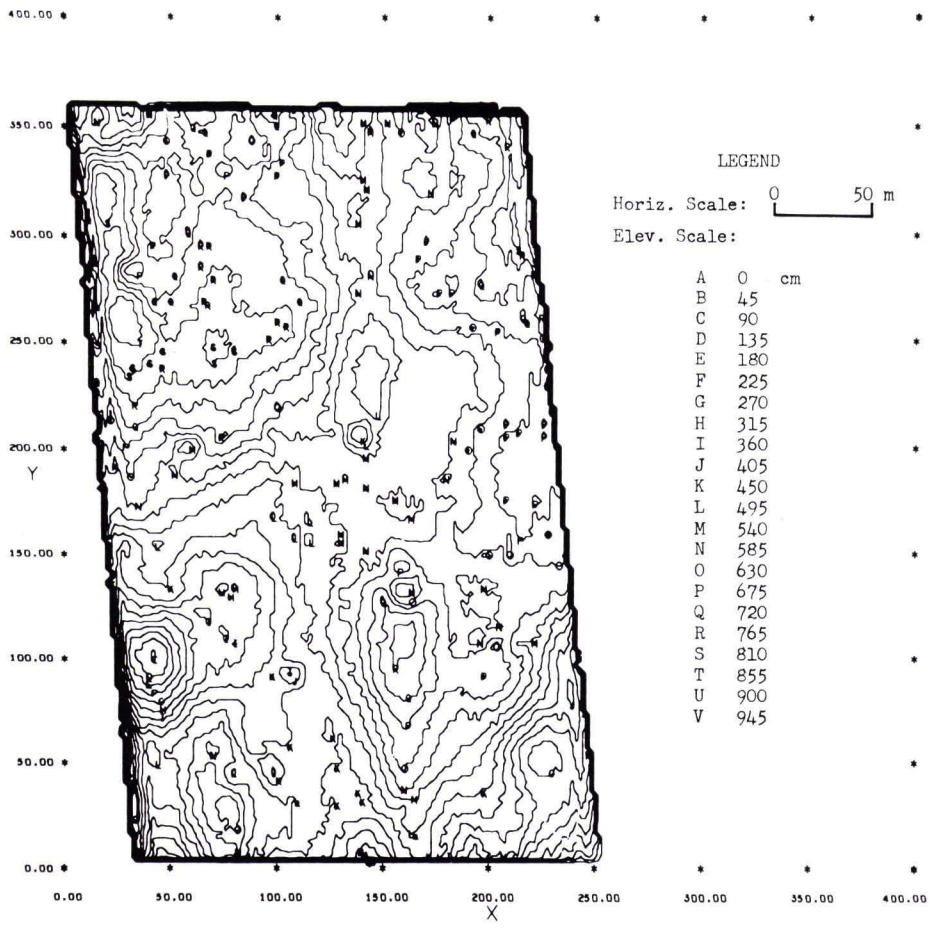

FIG. 8. Rectified contour map of P-1 picture (1005) from Ranger VIII.

This method of topographic mapping has proved quite useful for the monoscopic lunar photography obtained by the three Rangers. It is clear that many other spacecraft systems have or will obtain mainly monoscopic photography so that the present method could be of use in extracting topographic data from the pictures. A detailed investigation of the general equation derived herein with respect to specific photometric properties could yield useful results for terrestrial and planetary photography as well as lunar photography.

ACKNOWLEDGMENTS

The author wishes to express his gratitude to Dr. R. Nathan who established the digital video data processing program at the Jet Propulsion Laboratory and to Mr. F. Lyle, Mr. H. Frieden, Dr. W. Kirk and Mr. P. Jepsen of Mesa Scientific who provided invaluable programming support. He is further indebted to Mr. G. Smith for helpful discussion in computerizing the calculations and to Messrs. D. Willingham and W. Kirhofer for providing the necessary camera pointing data for the Rangers.

REFERENCES

1. J. van Diggelen, "A Photometric Investigation of the Slopes and the Heights of the Ranges of Hills in the Maria of the Moon," *Bulletin of the Astronomical Institutes of the Netherlands*, Vol. XI, No. 423, July 26, 1951.
2. D. E. Willingham, The Lunar Reflectivity Model for Ranger Block III Analysis, *Technical Report 32-664*, Jet Propulsion Laboratory, Pasadena, California (Nov. 1964).